PAN ARCHIVES OF ACOUSTICS
Vol. 42, No. 4, pp. 735–742 (2017)

DOI: 10.1515/aoa-2017-0076

Using PWE/FE Method to Calculate the Band Structures of the Semi-Infinite PCs: Periodic in x-y Plane and Finite in z-direction

Denghui QIAN, Zhiyu SHI

State Key Laboratory of Mechanics and Control of Mechanical Structures
College of Aerospace Engineering
Nanjing University of Aeronautics and Astronautics
Yudao Street No.29, Nanjing, Jiangsu, 210016, China; e-mail: zyshi@nuaa.edu.cn

(*received January 13, 2017; accepted May 18, 2017*)

This paper introduces the concept of semi-infinite phononic crystal (PC) on account of the infinite periodicity in x-y plane and finiteness in z-direction. The plane wave expansion and finite element methods are coupled and formulized to calculate the band structures of the proposed periodic elastic composite structures based on the typical geometric properties. First, the coupled plane wave expansion and finite element (PWE/FE) method is applied to calculate the band structures of the Pb/rubber, steel/epoxy and steel/aluminum semi-infinite PCs with cylindrical scatters. Then, it is used to calculate the band structure of the Pb/rubber semi-infinite PC with cubic scatter. Last, the band structure of the rubber-coated Pb/epoxy three-component semi-infinite PC is calculated by the proposed method. Besides, all the results are compared with those calculated by the finite element (FE) method implemented by adopting COMSOL Multiphysics. Numerical results and further analysis demonstrate that the proposed PWE/FE method has strong applicability and high accuracy.

Keywords: semi-infinite phononic crystal; coupled plane wave expansion and finite element method; band structure.

1. Introduction

Over the past decades, the artificial periodic elastic composite materials called as PCs have been attracting great interest (Sigalas, Economou, 1993; Sigalas *et al.*, 2005; Yan *et al.*, 2010a). PCs have many potential applications in filter, insulator, waveguide and sensor of acoustics and vibration on account of the existence of acoustic/elastic band gaps (Wu *et al.*, 2005; Benchabane *et al.*, 2006; Mohammadi *et al.*, 2009). Brag scattering (Sigalas, Economou, 1992; Zhang *et al.*, 2003) and locally resonant (Liu *et al.*, 2000b; Hirsekorn *et al.*, 2004) are developed as the two main mechanisms for the creation of band gaps, which the frequency range of band gaps based on the first mechanism is almost two orders of magnitude higher than that based on the second mechanism (Liu *et al.*, 2000b). Recently, the design ideas of both the Brag PCs and locally resonant PCs have been widely implemented in some basic elastic structures such as rods, beams and plates (Wang *et al.*, 2006; Ma *et al.*, 2014; Hsu, Wu, 2007; Xiao *et al.*, 2008; Oudich *et al.*, 2010; Zhao *et al.*, 2016; Li *et al.*, 2015; 2016; Qian, Shi, 2016; 2017a; Yu *et al.*, 2006).

In general, whatever the bandgap property research or the application research, the researches on calculation methods are fundamental. For now, several methods have been developed, which include the transfer matrices (TM) method (Hou *et al.*, 2004; Yan *et al.*, 2010b), the finite difference time domain (FDTD) method (Sigalas, Garcia, 2000; Cao *et al.*, 2004b), the multiple scattering theory (MST) method (Mei *et al.*, 2003; Liu *et al.*, 2000a), the lump mass (LM) method (Wang *et al.*, 2004; 2005), the plane wave expansion (PWE) method (Kushwaha *et al.*, 1994; Kushwaha, Halevi, 1997; Hsu, Wu, 2006; Xiao *et al.*, 2012) and the finite element (FE) method (Orris, Petyt, 1974; Åberg, Gudmundson, 1997). The MST method is efficient to calculate the band structures of PCs, but the shapes of the scatters are limited in cylinder and sphere. The FDTD method is very flexible in handling different kinds of PCs, but it is generally rather time consuming, especially for three dimensional systems. In recent years, with the

emergence of the commercial software COMSOL Multiphysics, FE method has been widely applied to the research on PCs (Ma *et al.*, 2014; Oudich *et al.*, 2010; Zhao *et al.*, 2016; Li *et al.*, 2015; 2016). The FE method can be applied to deal with almost all kinds of PCs, but it also consumes too long time particularly when the system is complex. The PWE method exhibits flexibility and high efficiency in handling different types of PCs, but has convergence problems when dealing with systems of either very high or very low filling ratios, or of large elastic mismatch. In addition, for the proposed semi-infinite PCs in this paper, only the FE method can be applied to calculate the band structures, most of the traditional methods including the PWE method are not applicable.

In this paper, we propose the semi-infinite periodic elastic composite structure named as semi-infinite PC based on some engineering components. In allusion to the periodicity in x-y plane and finiteness in z-direction, the theories of plane wave expansion and finite element division are coupled (Qian, Shi, 2017b) to describe the displacement field, and the PWE/FE method is presented to calculate the band structures of the semi-infinite PCS. In order to illustrate the applicability of the proposed method to different solid semi-infinite PCs with kinds of materials, the band structures of the Pb/rubber, steel/epoxy and steel/aluminum semi-infinite PCs are calculated respectively. In order to illustrate the applicability of the proposed method to semi-infinite PCs with different shapes of scatters, the band structures of the Pb/rubber semi-infinite PCs with cylindrical and cubic scatters are displayed respectively. Beside, in order to reveal that the proposed method is applicable to calculate not only two-component semi-infinite PCs but also three-component semi-infinite PCs, both the band structures of the Pb/rubber two-component semi-infinite PC and rubber-coated Pb/epoxy three-component semi-infinite PC are calculated and displayed. In addition, in order to illustrate the accuracy of the proposed method, all the band structures calculated by the PWE/FE method are compared with those calculated by the FE method implemented by adopting COMSOL Multiphysics.

2. Model and formulations

Consider a 3D semi-infinite PC by periodically etching holes in a solid matrix and then filling them with scatters in the x-y plane, as sketched in Fig. 1a. Here, the length of the elastic medium in z-direction is finite H with no periodicity, and the lattice constant is a as shown in Fig. 1b. Because of the infinite periodicity and the finiteness of the elastic medium in x-y plane and z-direction, the theories of plane wave expansion (Kushwaha *et al.*, 1994; Kushwaha, Halevi, 1997) and finite element (Eslami *et al.*, 2013) are applied respectively.

By representing the displacement field with the interpolating function in an element in z-direction and the spatial Fourier expansion in x-y plane, it can be written as:

$$\{u\} = [N_z]\,[N_{xy}]\,\{\delta^e\} = [N]\,\{\delta^e\}\,, \tag{1}$$

where $\{u\} = \left\{ u \;\; v \;\; w \right\}^{\mathrm{T}}$ denotes the displacement vector, $\{\delta^e\}$ represents the nodal displacement vector in an element, $[N_z]$ is the shape function matrix along z-direction, $[N_{xy}]$ is the spatial Fourier expansion matrix in x-y plane, and $[N] = [N_z]\,[N_{xy}]$ is the coupled spatial Fourier expansion and shape function matrix. When the interpolating function is linear, the matrixes can be written as follows:

$$[N_z] = \begin{bmatrix} a^* & 0 & 0 & b^* & 0 & 0 \\ 0 & a^* & 0 & 0 & b^* & 0 \\ 0 & 0 & a^* & 0 & 0 & b^* \end{bmatrix}, \tag{2}$$

where

$$a^* = \frac{z - z_2}{z_1 - z_2}, \qquad b^* = -\frac{z - z_1}{z_1 - z_2},$$

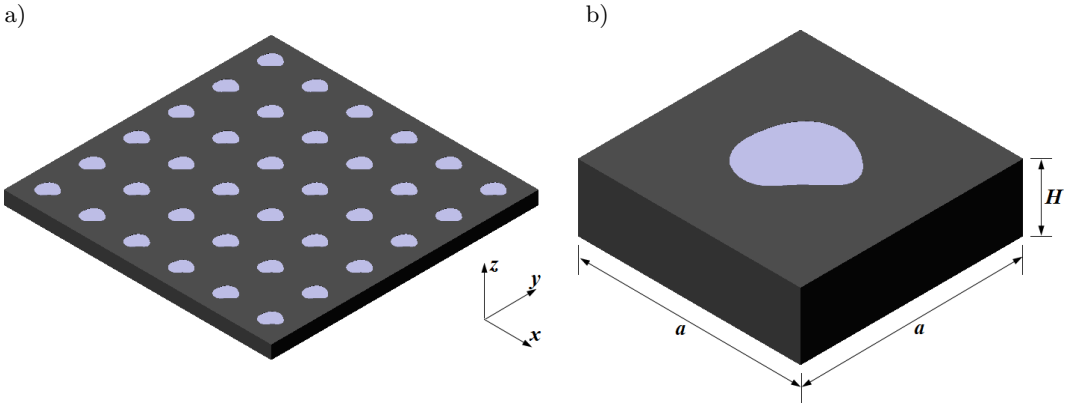

Fig. 1. a) The 3D semi-infinite PC infinitely periodic in x-y plane and finite in z-direction, b) its unit cell, a is the lattice constant, and H is the length in z-direction.

$$[N_{xy}]=\begin{bmatrix}\{GK\} & 0 & 0 & 0 & 0 & 0\\ 0 & \{GK\} & 0 & 0 & 0 & 0\\ 0 & 0 & \{GK\} & 0 & 0 & 0\\ 0 & 0 & 0 & \{GK\} & 0 & 0\\ 0 & 0 & 0 & 0 & \{GK\} & 0\\ 0 & 0 & 0 & 0 & 0 & \{GK\}\end{bmatrix}, \quad (3)$$

$$\{\delta^e\}=\left\{\{u^1\}\ \{v^1\}\ \{w^1\}\ \{u^2\}\ \{v^2\}\ \{w^2\}\right\}^{\mathrm{T}}, \quad (4)$$

where

$$\{GK\}=\left\{e^{i(\mathbf{G}_1+k)r}\ e^{i(\mathbf{G}_2+k)r}\ \cdots\ e^{i(\mathbf{G}_N+k)r}\right\}, \quad (5)$$

$$\left\{u^1\right\}=\left\{u_k(\mathbf{G}_1)u_z^1\ u_k(\mathbf{G}_2)u_z^1\ \cdots\ u_k(\mathbf{G}_N)u_z^1\right\}, \quad (6)$$

$$\left\{v^1\right\}=\left\{v_k(\mathbf{G}_1)v_z^1\ v_k(\mathbf{G}_2)v_z^1\ \cdots\ v_k(\mathbf{G}_N)v_z^1\right\}, \quad (7)$$

$$\left\{w^1\right\}=\left\{w_k(\mathbf{G}_1)w_z^1\ w_k(\mathbf{G}_2)w_z^1\ \cdots\ w_k(\mathbf{G}_N)w_z^1\right\}, \quad (8)$$

$$\left\{u^2\right\}=\left\{u_k(\mathbf{G}_1)u_z^2\ u_k(\mathbf{G}_2)u_z^2\ \cdots\ u_k(\mathbf{G}_N)u_z^2\right\}, \quad (9)$$

$$\left\{v^2\right\}=\left\{v_k(\mathbf{G}_1)v_z^2\ v_k(\mathbf{G}_2)v_z^2\ \cdots\ v_k(\mathbf{G}_N)v_z^2\right\}, \quad (10)$$

$$\left\{w^2\right\}=\left\{w_k(\mathbf{G}_1)w_z^2\ w_k(\mathbf{G}_2)w_z^2\ \cdots\ w_k(\mathbf{G}_N)w_z^2\right\}. \quad (11)$$

Here, z_1 and z_2 represent the range of element in z-direction. k and $\mathbf{G}_i$ $(i=1,2,\cdots,N)$ are the 2D Bloch wave vector limited in the irreducible first Brillouin zone (1BZ) and the reciprocal-lattice vector, respectively. N is the number of reciprocal-lattice vectors.

According to the fundamental equations of the elastodynamics (Eslami *et al.*, 2013), the relations between the strain/stress in an element and the nodal displacements can be expressed as:

$$\{\varepsilon\} = [\nabla][N]\{\delta^e\} = [B]\{\delta^e\}, \quad (12)$$

$$\{\sigma\} = [D][B]\{\delta^e\}, \quad (13)$$

where $\{\varepsilon\}$ and $\{\sigma\}$ denote the strain and stress vectors, respectively. $[\nabla]$, $[B]=[\nabla][N]$ and $[D]$ named as differential operator matrix, geometric matrix and elastic matrix are expressed as:

$$[\nabla]=\begin{bmatrix}\dfrac{\partial}{\partial x} & 0 & 0\\ 0 & \dfrac{\partial}{\partial y} & 0\\ 0 & 0 & \dfrac{\partial}{\partial z}\\ 0 & \dfrac{\partial}{\partial z} & \dfrac{\partial}{\partial y}\\ \dfrac{\partial}{\partial z} & 0 & \dfrac{\partial}{\partial x}\\ \dfrac{\partial}{\partial y} & \dfrac{\partial}{\partial x} & 0\end{bmatrix}, \quad (14)$$

$$[D]=\begin{bmatrix}\alpha & \lambda & \lambda & 0 & 0 & 0\\ \lambda & \alpha & \lambda & 0 & 0 & 0\\ \lambda & \lambda & \alpha & 0 & 0 & 0\\ 0 & 0 & 0 & \mu & 0 & 0\\ 0 & 0 & 0 & 0 & \mu & 0\\ 0 & 0 & 0 & 0 & 0 & \mu\end{bmatrix}, \quad (15)$$

where λ and μ are the Lame constants of the elastic medium, and $\alpha=\lambda+2\mu$.

Taking advantage of the periodicity of the medium we expand the elastic matrix $[D]$ in Fourier series:

$$[D]=\sum_{\mathbf{G}}\begin{bmatrix}\alpha(\mathbf{G}) & \lambda(\mathbf{G}) & \lambda(\mathbf{G}) & 0 & 0 & 0\\ \lambda(\mathbf{G}) & \alpha(\mathbf{G}) & \lambda(\mathbf{G}) & 0 & 0 & 0\\ \lambda(\mathbf{G}) & \lambda(\mathbf{G}) & \alpha(\mathbf{G}) & 0 & 0 & 0\\ 0 & 0 & 0 & \mu(\mathbf{G}) & 0 & 0\\ 0 & 0 & 0 & 0 & \mu(\mathbf{G}) & 0\\ 0 & 0 & 0 & 0 & 0 & \mu(\mathbf{G})\end{bmatrix}e^{i\mathbf{G}\mathbf{r}}. \quad (16)$$

In addition, the density ρ can also be expanded in Fourier series as:

$$\rho=\sum_{\mathbf{G}}\rho(\mathbf{G})\,\mathrm{e}^{i\mathbf{G}\mathbf{r}}. \quad (17)$$

Here,

$$g(\mathbf{G})=\frac{1}{S}\iint_S g(\mathbf{r})\,\mathrm{e}^{i\mathbf{G}\mathbf{r}}\,\mathrm{d}^2\mathbf{r} \quad (g=\alpha,\lambda,\mu,\rho). \quad (18)$$

According to the variation principle (Eslami *et al.*, 2013), the stiffness matrix and mass matrix of the elastic medium are obtained by coupling the element stiffness matrix and element mass matrix, which can be written as:

$$[K^e] = \iiint_{V^e}[B]^T[D][B]\,\mathrm{d}V, \quad (19)$$

$$[M^e] = \iiint_{V^e}\rho[N]^T[N]\,\mathrm{d}V, \quad (20)$$

where $[K^e]$ and $[M^e]$ represent the element stiffness matrix and element mass matrix, respectively. Particularly, the integral $\iiint_{V^e}(\cdot)\,\mathrm{d}V$ in the x-y plane is in the infinite domain.

$[K^e]$ and $[M^e]$ can be expressed in the form of block matrix as follows:

$$[K^e]=\begin{bmatrix}[K^e]_{11} & [K^e]_{12} & [K^e]_{13} & [K^e]_{14} & [K^e]_{15} & [K^e]_{16}\\ [K^e]_{21} & [K^e]_{22} & [K^e]_{23} & [K^e]_{24} & [K^e]_{25} & [K^e]_{26}\\ [K^e]_{31} & [K^e]_{32} & [K^e]_{33} & [K^e]_{34} & [K^e]_{35} & [K^e]_{36}\\ [K^e]_{41} & [K^e]_{42} & [K^e]_{43} & [K^e]_{44} & [K^e]_{45} & [K^e]_{46}\\ [K^e]_{51} & [K^e]_{52} & [K^e]_{53} & [K^e]_{54} & [K^e]_{55} & [K^e]_{56}\\ [K^e]_{61} & [K^e]_{62} & [K^e]_{63} & [K^e]_{64} & [K^e]_{65} & [K^e]_{66}\end{bmatrix}, \quad (21)$$

$$[M^e]=\begin{bmatrix} [M^e]_{11} & [M^e]_{12} & [M^e]_{13} & [M^e]_{14} & [M^e]_{15} & [M^e]_{16} \\ [M^e]_{21} & [M^e]_{22} & [M^e]_{23} & [M^e]_{24} & [M^e]_{25} & [M^e]_{26} \\ [M^e]_{31} & [M^e]_{32} & [M^e]_{33} & [M^e]_{34} & [M^e]_{35} & [M^e]_{36} \\ [M^e]_{41} & [M^e]_{42} & [M^e]_{43} & [M^e]_{44} & [M^e]_{45} & [M^e]_{46} \\ [M^e]_{51} & [M^e]_{52} & [M^e]_{53} & [M^e]_{54} & [M^e]_{55} & [M^e]_{56} \\ [M^e]_{61} & [M^e]_{62} & [M^e]_{63} & [M^e]_{64} & [M^e]_{65} & [M^e]_{66} \end{bmatrix}. \quad (22)$$

Here, take $[K^e]_{11}$ as an example. $[K^e]_{11}$ can be obtained from equation (16) as:

$$\begin{aligned}[K^e]_{11} &= \iiint_{V^e} \sum_{\mathbf{G}} \alpha(\mathbf{G})\, \mathrm{e}^{i\mathbf{Gr}} [B_{11}]^{\mathrm{T}} [B_{11}]\, \mathrm{d}V \\ &+ \iiint_{V^e} \sum_{\mathbf{G}} \mu(\mathbf{G})\, \mathrm{e}^{i\mathbf{Gr}} [B_{51}]^{\mathrm{T}} [B_{51}]\, \mathrm{d}V \\ &+ \iiint_{V^e} \sum_{\mathbf{G}} \mu(\mathbf{G})\, \mathrm{e}^{i\mathbf{Gr}} [B_{61}]^{\mathrm{T}} [B_{61}]\, \mathrm{d}V. \quad (23)\end{aligned}$$

The first item of $[K^e]_{11}$ can be further written as:

$$\begin{aligned}&\iiint_{V^e} \sum_{\mathbf{G}} \alpha(\mathbf{G})\, \mathrm{e}^{i\mathbf{Gr}} [B_{11}]^{\mathrm{T}} [B_{11}]\, \mathrm{d}V \\ &= \iiint_{V^e} \sum_{\mathbf{G}} \alpha(\mathbf{G})\, \mathrm{e}^{i\mathbf{Gr}} \left(\frac{z-z_2}{z_1-z_2}\right)^2 \{GK\}_{,x}^{\mathrm{T}} \{GK\}_{,x}\, \mathrm{d}V \\ &= \int_{z_1}^{z_2} \left(\frac{z-z_2}{z_1-z_2}\right)^2 \cdot \begin{bmatrix} [K_1^e]_{1111} & [K_1^e]_{1112} & \cdots & [K_1^e]_{111N} \\ [K_1^e]_{1121} & [K_1^e]_{1122} & \cdots & [K_1^e]_{112N} \\ \vdots & \vdots & \ddots & \vdots \\ [K_1^e]_{11N1} & [K_1^e]_{11N2} & \cdots & [K_1^e]_{11NN} \end{bmatrix} \mathrm{d}z, \quad (24)\end{aligned}$$

where

$$\begin{aligned}[K_1^e]_{11lm} &= \iint_S \sum_{\mathbf{G}} \alpha(\mathbf{G})\, e^{i\mathbf{Gr}} (\mathbf{G}_l + \mathbf{k})_x \\ &\quad \cdot (\mathbf{G}_m + \mathbf{k})_x\, \mathrm{e}^{i(-\mathbf{G}_l+\mathbf{G}_m)\mathbf{r}}\, \mathrm{d}S \\ &= \sum_{\mathbf{G}} \alpha(\mathbf{G}) (\mathbf{G}_l+\mathbf{k})_x (\mathbf{G}_m+\mathbf{k})_x\, \delta_{\mathbf{G},(-\mathbf{G}_l+\mathbf{G}_m)} \\ &= \alpha(\mathbf{G}_m - \mathbf{G}_l) (\mathbf{G}_l + \mathbf{k})_x (\mathbf{G}_m + \mathbf{k})_x \\ &\quad (l, m = 1, 2, \cdots, N). \quad (25)\end{aligned}$$

Similar to the first item of $[K^e]_{11}$, all the block matrixes of $[K^e]$ and $[M^e]$ can be obtained. Particularly when the cross section along x-y plane is constant in z-direction, the integral $\int_{z_1}^{z_2} (\cdot)\, \mathrm{d}z$ can be obtained analytically.

In addition, according to the variation principle (Eslami *et al.*, 2013), the equation of motion can be written as:

$$\left([K] - \omega^2 [M]\right) = \mathbf{0}, \quad (26)$$

where $[K] = \sum_e [K^e]$ and $[M] = \sum_e [M^e]$ represent the stiffness matrix and mass matrix of the elastic medium.

Equation (26) represents a generalized eigenvalue problem for ω^2. By solving the equation for each 2D Bloch wave vector limited in the irreducible first Brillouin zone (1BZ), the band structure can be obtained finally.

3. Numerical results and analyses

3.1. Two-component semi-infinite PC with cylindrical scatter

The semi-infinite PC is formed with Pb cylinders arranged in a square lattice in rubber matrix, as shown in Fig. 2a. The materials' parameters are shown in Table 1. The lattice constant a, height H and scatter radius R are displayed in Table 2.

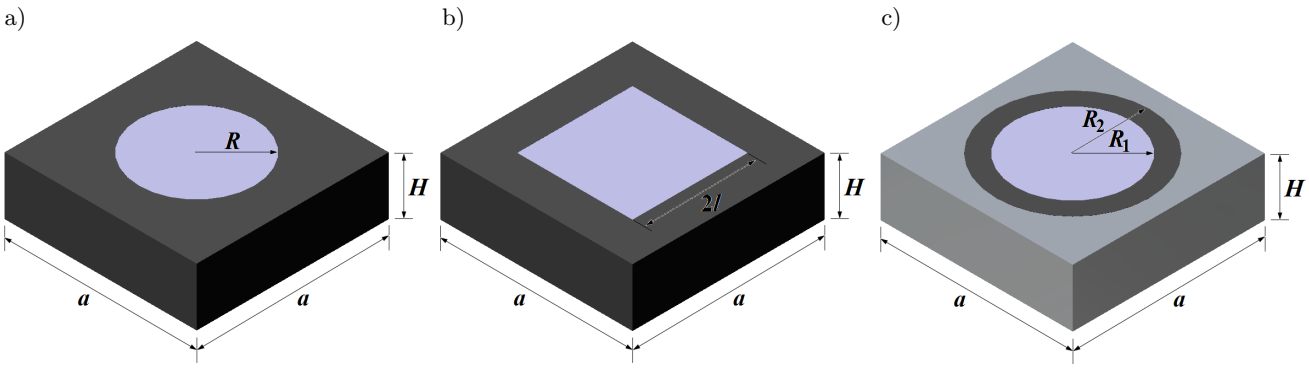

Fig. 2. a) The two-component semi-infinite PC with cylindrical scatter, b) the two-component semi-infinite PC with cubic scatter, c) and the three-component semi-infinite PC with cylindrical scatter.

Table 1. Materials' parameters used in calculations.

Material	Mass density [kg/m^3]	Young's modulus [10^{10} N/m^2]	Poission's ratio
Epoxy	1180	0.435	0.368
Rubber	1300	1.175e-5	0.469
Pb	11600	4.08	0.37
Steel	7780	21.06	0.3
Aluminum	2730	7.76	0.352

Table 2. Geometric parameters used in calculations.

a [m]	H [m]	R [m]	l [m]	R_1 [m]	R_2 [m]
0.02	0.02	0.008	0.008	0.008	0.009

In this section, three groups of examples are displayed. In addition, to check the accuracy of the formalism and program, the band structure of each example calculated by the proposed approach (PWE/FEM) is compared to that calculated by FEM, which is implemented by adopting the commercial software, COMSOL Multiphysics. In order to improve the calculation accuracy, the improved PWE method (Cao *et al.*, 2004a) is applied to PWE/FE method.

Here, equation (18) can be written as:

$$g(\mathbf{G}) = \begin{cases} g_{\mathrm{A}} f + g_{\mathrm{B}}(1-f), & \mathbf{G} = 0 \\ (g_{\mathrm{A}} - g_{\mathrm{B}})\, P(\mathbf{G}), & \mathbf{G} \neq 0 \end{cases} \quad (g = \alpha, \lambda, \mu, \rho), \tag{27}$$

where subscript A and B denote the scatter (Pb) and matrix (rubber) respectively. $f = \pi R^2/a^2$ represents the filling ratio, and $P(\mathbf{G})$ can be expressed as:

$$P(\mathbf{G}) = 2f\frac{J_1(GR)}{GR}, \tag{28}$$

where J_1 is the Bessel function of the first kind of order 1, and $G = |\mathbf{G}|$.

Figure 3 displays the band structure of the semi-infinite phononic crystal with the unit cell shown in Fig. 2a. Here, $N = (5 \cdot 2 + 1)^2$ plane waves in x-y plane and 5 elements in z-direction are chosen. As a comparison, the band structure calculated by FEM is also shown. As shown in the figure, two locally resonant band gaps are formed (the gray area in Fig. 3). Besides, by comparing the band structures calculated by the two methods, they are in good agreement under 450 Hz. Thus, for PWE/FEM, only a small number of plane waves in x-y plane and elements in z-direction are needed to obtain the accurate band gap, which is very efficient.

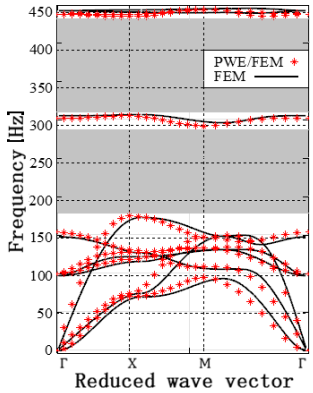

Fig. 3. Band structures of the Pb/rubber two-component semi-infinite PC with cylindrical scatter calculated by PWE/FEM and FEM.

In order to illustrate the applicability of the proposed method in this paper, the band structures of different semi-infinite PCs formed by different materials are calculated. Figures 4a and 4b show the band structures of steel/epoxy and steel/aluminum semi-infinite PCs respectively with the same geometric parameters as those in the example shown in Fig. 3. The materials' parameters are displayed in Table 1. From Fig. 4a, the Bragg scattering band gaps are formed in steel/epoxy semi-infinite PC. But Fig. 4b show that no band gaps can be formed in steel/aluminum semi-infinite phononic crystal. In addition, both the band structures of the two semi-infinite PCs calculated by PWE/FEM agree very well with those calculated by FEM. Therefore, the proposed PWE/FEM can be applied for different solid semi-infinite phononic crystals with kinds of materials.

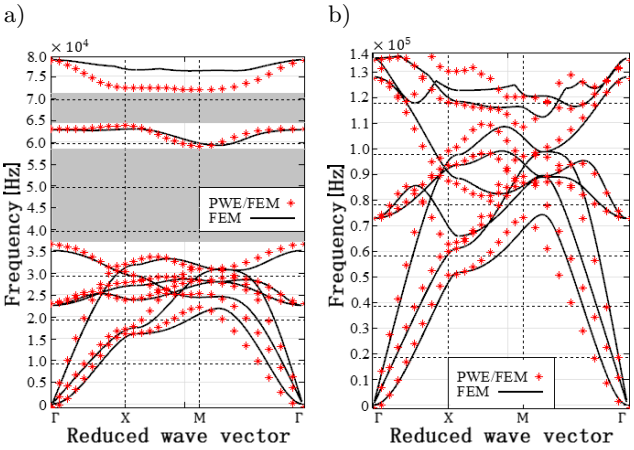

Fig. 4. Band structures of the steel/epoxy and steel/aluminum two-component semi-infinite PCs with cylindrical scatter calculated by PWE/FEM and FEM.

3.2. Two-component semi-infinite PC with cubic scatter

In order to reveal the applicability of PWE/FEM for calculating the band structure of the semi-infinite PC with different shapes of scatters, the PC with Pb cuboids arranged in rubber matrix is formed, as shown in Fig. 2b. The materials' parameters and geometric parameters are displayed in Table 1 and Table 2, respectively.

Here, in Eq. (27), $f = (2l)^2/a^2$ and $P(\mathbf{G})$ can be written as:

$$P(\mathbf{G}) = \begin{cases} f\dfrac{\sin(G_y l)}{G_y l}, & G_x = 0, G_y \neq 0, \\ f\dfrac{\sin(G_x l)}{G_x l}, & G_y = 0, G_x \neq 0, \\ f\dfrac{\sin(G_x l)}{G_x l}\dfrac{\sin(G_y l)}{G_y l}, & G_x G_y \neq 0. \end{cases} \quad (29)$$

The band structures of the semi-infinite PC with the unit cell shown in Fig. 2b calculated by PWE/FEM and FEM are both shown in Fig. 5. Here, the same numbers of plane waves and elements as the example in Fig. 3 are used. In the figure, by comparing the band structures calculated by the two methods, they are in good agreement under 650 Hz only except for the flat band around 550 Hz. Thus, the proposed method is completely applicable for dealing with the two-component semi-infinite PC with cubic scatter. By comparing Fig. 5 with Fig. 3, we can conclude that the proposed method is applicable to semi-infinite PCs with different shapes of scatters.

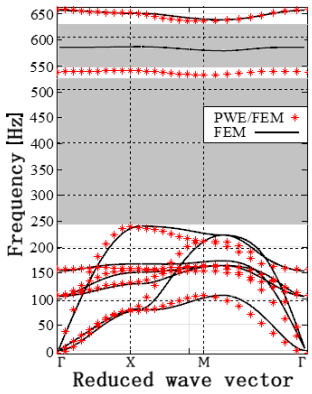

Fig. 5. Band structures of the Pb/rubber two-component semi-infinite PC with cubic scatter calculated by PWE/FEM and FEM.

3.3. Three-component semi-infinite PC with cylindrical scatter

In order to reveal that the proposed method in this paper can be not only used to calculate the band structure of the two-component semi-infinite PC but also applicable to the three-component semi-infinite PC, the rubber-coated Pb cylinders are arranged in a square lattice in epoxy matrix, as shown in Fig. 2c. The materials' parameters are shown in Table 1. The geometric parameters are displayed in Table 2.

Here, equation (18) can be written as:

$$g(\mathbf{G}) = \begin{cases} g_A f_1 + g_B f_2 + g_C(1 - f_1 - f_2), & \mathbf{G} = 0, \\ (g_A - g_B)P_1(\mathbf{G}) + (g_B - g_C)P_2(\mathbf{G}), & \mathbf{G} \neq 0 \end{cases}$$
$$(g = \alpha, \lambda, \mu, \rho), \quad (30)$$

where subscript A, B and C denote the Pb layer, rubber layer and epoxy layer, respectively. $f_1 = \pi R_1^2/a^2$ and $f_2 = \pi(R_2^2 - R_1^2)/a^2$ represent the filling ratios of Pb layer and rubber layer separately. $P_1(\mathbf{G})$ and $P_2(\mathbf{G})$ can be expressed as:

$$P_1(\mathbf{G}) = 2f_1\frac{J_1(GR_1)}{GR_1}, \quad (31)$$

$$P_2(\mathbf{G}) = 2(f_1 + f_2)\frac{J_1(GR_2)}{GR_2}. \quad (32)$$

Figure 6 shows the band structures of the three-component semi-infinite PC calculated by PWE/FEM and FEM. Here, $N = (20 \cdot 2 + 1)^2$ plane waves are used to improve the convergence. As shown in the figure, a narrow locally resonant band gap is formed around 500 Hz, and the band structures calculated by the two methods agree well under 2600 Hz. By comparing Fig. 6 with Fig. 3, what can be concluded is that the proposed method can be applied to not only the two-component semi-infinite PC but also the three-component semi-infinite PC.

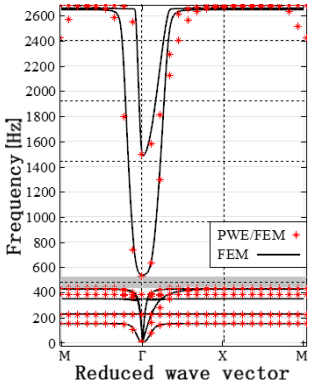

Fig. 6. Band structures of the rubber-coated Pb/epoxy three-component semi-infinite PC with cylindrical scatter calculated by PWE/FEM and FEM.

4. Conclusions

In this paper, we formulize the PWE/FE method to calculate the band structures of the proposed semi-infinite PCs. All the band structures calculated by the proposed method are compared to the ones calculated by FE method, which are in good agreement. In addition, three groups of examples are calculated and displayed to illustrate the applicability of the proposed method:

1) By comparing the band structures of the Pb/rubber, steel/epoxy and steel/aluminum two-component semi-infinite PCs with cylindrical scatter, we conclude that PWE/FE method is applicable to different solid semi-infinite PCs with kinds of materials.
2) By comparing the band structures of the Pb/rubber two-component semi-infinite PCs with cylindrical and cubic scatters, it can be concluded that

the proposed method is applicable to semi-infinite PCs with different shapes of scatters.

3) By comparing the band structures of the Pb/rubber two-component semi-infinite PC and rubber-coated Pb/epoxy three-component semi-infinite PC with cylindrical scatter, what can be concluded is that the proposed method is applicable to not only two-component semi-infinite PCs but also three-component semi-infinite PCs.

All the results of the investigation verify the strong applicability and high accuracy of PWE/FE method, which provide a new method for dealing with the semi-infinite periodic elastic composite structures with the infinite periodicity in x-y plane and finiteness in z-direction.

Acknowledgments

This research is supported by the National Natural Science Foundation of China through Grant No. 11172131, the Research Fund of State Key Laboratory of Mechanics and Control of Mechanical Structures, Nanjing University of Aeronautics and Astronautics (Grant No. 0515G01) and the Research Fund of Science and Technology Project of Jiangsu Province (Grant No. 2015003-01).

References

1. Åberg M., Gudmundson P. (1997), *The usage of standard finite element codes for computation of dispersion relations in materials with periodic microstructure*, Journal of the Acoustical Society of America, **102**, 4, 2007–2013.
2. Benchabane S., Khelif A., Rauch J.Y. *et al.* (2006), *Evidence for complete surface wave band gap in a piezoelectric phononic crystal*, Physical Review E: Statistical Nonlinear & Soft Matter Physics, **73**, 2, 95–104.
3. Cao Y., Hou Z., Liu Y. (2004a), *Convergence problem of plane-wave expansion method for phononic crystals*, Physics Letters A, **327**, 2–3, 247–253.
4. Cao Y., Hou Z., Liu Y. (2004b), *Finite difference time domain method for band-structure calculations of two-dimensional phononic crystals*, Solid State Communications, **132**, 8, 539–543.
5. Eslami M.R., Hetnarski R.B., Ignaczak J., Noda N., Sumi N., Tanigawa Y. (2013), *Variational Principles of Elastodynamics.* In: *Theory of Elasticity and Thermal Stresses. Solid Mechanics and Its Applications*, Vol. 197, pp. 127–149. Springer, Dordrecht. https://doi.org/10.1007/978-94-007-6356-2_5.
6. Hirsekorn M., Delsanto P.P., Batra N.K. *et al.* (2004), *Modelling and simulation of acoustic wave propagation in locally resonant sonic materials*, Ultrasonics, **42**, 1, 231–235.
7. Hou Z., Fu X., Liu Y. (2004), *Calculational method to study the transmission properties of phononic crystals*, Physical Review B: Condensed Matter, **70**, 1, 2199–2208.
8. Hsu J.C., Wu T.T. (2006), *Efficient formulation for band-structure calculations of two-dimensional phononic-crystal plates*, Physical Review B: Condensed Matter, **74**, 74, 2952–2961.
9. Hsu J.C., Wu T.T. (2007), *Lamb waves in binary locally resonant phononic plates with two-dimensional lattices*, Applied Physics Letters, **90**, 20, 201904–201904-3.
10. Kushwaha M.S., Halevi P. (1997), *Stop bands for cubic arrays of spherical balloons*, Journal of the Acoustical Society of America, **101**, 1, 619–622.
11. Kushwaha M.S., Halevi P., Martínez G., Dobrzynski L., Djafari-Rouhani B. (1994), *Theory of acoustic band structure of periodic elastic composites*, Physical Review B: Condensed Matter, **49**, 4, 2313–2322.
12. Li S., Chen T., Wang X., Li Y., Chen W. (2016), *Expansion of lower-frequency locally resonant band gaps using a double-sided stubbed composite phononic crystals plate with composite stubs*, Physics Letters A, **380**, 25–26, 2167–2172.
13. Li Y., Chen T., Wang X., Xi Y., Liang Q. (2015), *Enlargement of locally resonant sonic band gap by using composite plate-type acoustic metamaterial*, Physics Letters A, **379**, 5, 412–416.
14. Liu Z., Chan C.T., Sheng P., Goertzen A.L., Page J.H. (2000a), *Elastic wave scattering by periodic structures of spherical objects: Theory and experiment*, Physical Review B, **62**, 4, 2446–2457.
15. Liu Z., Zhang X., Mao Y. *et al.* (2000b), *Locally resonant sonic materials*, Science, **289**, 5485, 1734–1736.
16. Ma J., Hou Z., Assouar B.M. (2014), *Opening a large full phononic band gap in thin elastic plate with resonant units*, Journal of Applied Physics, **115**, 9, 093508–093508-5.
17. Mei J., Liu Z., Shi J., Decheng T. (2003), *Theory for elastic wave scattering by a two-dimensional periodical array of cylinders: An ideal approach for band-structure calculations*, Physical Review B, **67**, 24, 841–845.
18. Mohammadi S., Eftekhar A.A., Hunt W.D., Adibi A. (2009), *High-Q micromechanical resonators in a two-dimensional phononic crystal slab*, Applied Physics Letters, **94**, 5, 051906–051906-3.
19. Orris R.M., Petyt M. (1974), *A finite element study of harmonic wave propagation in periodic structures*, Journal of Sound & Vibration, **33**, 2, 223–236.
20. Oudich M., Li Y., Assouar B.M., Hou Z. (2010), *A sonic band gap based on the locally resonant phononic plates with stubs*, New Journal of Physics, **12**, 2, 201–206.
21. Qian D., Shi Z. (2016), *Bandgap properties in locally resonant phononic crystal double panel structures with periodically attached spring-mass resonators*, Physics Letters A, **380**, 41, 3319–3325.

22. Qian D., Shi Z. (2017a), *Bandgap properties in simplified model of composite locally resonant phononic crystal plate*, Physics Letters A, **381**, 40, 3505–3513.

23. Qian D., Shi Z. (2017b), *Using PWE/FE method to calculate the band structures of the semi-infinite beam-like PCs: periodic in z-direction and finite in x-y plane*, Physics Letters A, **381**, 17, 1516–1524.

24. Sigalas M., Economou E.N. (1993), *Band structure of elastic waves in two dimensional systems*, [J]. Solid State Communications, **86**, 3, 141–143.

25. Sigalas M., Kushwaha M.S., Economou E.N., Kafesaki M., Psarobas I.E., Steurer W. (2005), *Classical vibrational modes in phononic lattices: theory and experiment*, Zeitschrift für Kristallographie – Crystalline Materials, **220**, 9, 765–809.

26. Sigalas M.M., Economou E.N. (1992), *Elastic and acoustic wave band structure*, Journal of Sound and Vibration, **158**, 2, 377–382.

27. Sigalas M.M., Garcia N. (2000), *Theoretical study of three dimensional elastic band gaps with the finite-difference time-domain method*, Journal of Applied Physics, **87**, 6, 3122–3125.

28. Wang G., Wen J., Liu Y., Wen X. (2004), *Lumped-mass method for the study of band structure in two-dimensional phononic crystals*, Physical Review B, **69**, 18, 1324–1332.

29. Wang G., Wen J., Wen X. (2005), *Quasi-one-dimensional phononic crystals studied using the improved lumped-mass method: Application to locally resonant beams with flexural wave band gap*, Physical Review B, **71**, 10, 4302.

30. Wang G., Wen X., Wen J., Liu Y. (2006), *Quasi-One-Dimensional Periodic Structure with Locally Resonant Band Gap*, Journal of Applied Mechanics, **43**, 1, 167–170.

31. Wu T., Wu L.C., Huang Z.G. (2005), *Frequency band-gap measurement of two-dimensional air/silicon phononic crystals using layered slanted finger interdigital transducers*, Journal of Applied Physics, **97**, 9, 094916–094916-7.

32. Xiao W., Zeng G.W., Cheng Y.S. (2008), Flexural vibration band gaps in a thin plate containing a periodic array of hemmed discs, Applied Acoustics, **69**, 3, 255–261.

33. Xiao Y., Wen J., Wen X. (2012), *Flexural wave band gaps in locally resonant thin plates with periodically attached spring–mass resonators*, Journal of Physics D: Applied Physics, **45**, 19, 195401–195412(12).

34. Yan P., Vasseur J.O., Djafari-Rouhani B., Dobrzyński L., Deymier P.A. (2010a), *Two-dimensional phononic crystals: Examples and applications*, Surface Science Reports, **65**, 8, 229–291.

35. Yan Z.Z., Zhang C., Wang Y.S. (2010b), *Wave propagation and localization in randomly disordered layered composites with local resonances*, Wave Motion, **47**, 7, 409–420.

36. Yu D., Liu Y., Wang G., Zhao H., Qiu J. (2006), *Flexural vibration band gaps in Timoshenko beams with locally resonant structures*, Journal of Applied Physics, **100**, 12, 124901–124901-5.

37. Zhang X., Liu Z., Liu Y., Wu F. (2003), *Elastic wave band gaps for three-dimensional phononic crystals with two structural units*, Physics Letters A, 313, 5, 455–460.

38. Zhao H.J., Guo H.W., Gao M.X, Liu R.Q., Deng Z.Q. (2016), *Vibration band gaps in double-vibrator pillared phononic crystal plate*, Journal of Applied Physics, **119**, 1, 377.